RESEARCH ARTICLE

Synthesis of 1,4-dihydropyrrolo[3,2-b]pyrrole-containing donor-acceptor copolymers and their optoelectronic properties

Kenneth-John J. Bell¹ | Sina Sabury² | Vanessa Phan¹ | Ethan M. Wagner¹ | Allison M. Hawks¹ | Kimberley A. Bartlett¹ | Graham S. Collier^{1,3}

²School of Chemistry and Biochemistry, School of Materials Science and Engineering, Center for Organic Photonics and Electronics, Georgia Tech Polymers, Georgia Institute of Technology, Atlanta, Georgia, USA ³School of Polymer Science and Engineering, University of Southern Mississippi, Hattiesburg, Mississippi, USA

Correspondence

Graham S. Collier, School of Polymer Science and Engineering, University of Southern Mississippi, Hattiesburg, MS, 39406, USA

Email: graham.collier@usm.edu

Funding information

National Science Foundation, Grant/Award Number: 2203340; Kennesaw State University

Abstract

Donor-acceptor (D-A)-conjugated polymers have achieved promising performance metrics in numerous optoelectronic applications that continue to motivate studying structure-property relationships and discovering new materials. Here, the materials toolbox is expanded by synthesizing D-A copolymers where 1,4-dihydropyrrolo[3,2-b]pyrrole (DHPP) is directly incorporated into the main chain of D-A copolymers for the first time via direct heteroarylation polymerization. Notably, the synthetic complexity of DHPP-containing polymers coupled with thieno[3,2-b]pyrrole-4,6-dione (TPD) or 3,6-bis(2-thienyl)-2,5-dihydropyrrolo[3,4-c]pyrrole-1,4-dione (Th₂DPP) comonomers is calculated to be lower compared to many common conjugated polymers synthesized via direct arylation. The electron-rich nature of DHPPs when coupled with TPD or DPP enables optoelectronic properties to be manipulated, evident by measuring distinctly different absorbance and redox properties. Additionally, these D-A copolymers demonstrate their potential in organic electronic applications, such as electrochromics and organic photovoltaics. The reported DHPPalt-Th₂DPP copolymer is the first DHPP-based colored-to-transmissive electrochrome and achieves power conversion efficiencies of ~2.5% when incorporated into bulk heterojunction solar cells. Overall, the synthetic accessibility of DHPP monomers and their propensity to participate in robust polymerizations highlights the value of establishing structure-property relationships of an underutilized scaffold. These fundamental attributes serve to inform and advance efforts in the development of DHPP-containing copolymers for various applications.

KEYWORDS

conjugated polymers, optoelectronics, pyrrolopyrroles

1 | INTRODUCTION

Coupling electron-rich and electron-deficient comonomers to create copolymers via the donor-acceptor (D-A)

design approach enables tunability of optical and electrochemical properties for various organic electronic applications including organic photovoltaics (OPVs),¹ organic light emitting diodes (OLEDs),² and electrochromism.^{3,4}

¹Department of Chemistry and Biochemistry, Kennesaw State University, Kennesaw, Georgia, USA

However, attaining high-performance D-A copolymers typically require a large number of synthetic steps (upwards of 20 or more) which leads to a proportional increase in synthetic complexity.^{5–8} While the field has reached promising functional performances for D-A polymers, such as high power conversion efficiencies (18–19%) in OPV devices, studies of the synthetic complexity (including purification challenges), cost of starting monomers, and environmental impacts of the state-of-the-art donor-conjugated polymers have led to increased attention to considerations beyond power conversion efficiency values as the sole focus. 8,10-12 For example, Heeney and coworkers have developed nucleophilic aromatic substitution (SN_{Ar}) reactions that enable green solvent processing as well as access to easily scalable donor material for OPVs. 13-17 Furthermore, as highlighted by Lin and coworkers, developing low-cost materials is imperative for conjugated polymers to reach commercial viability. 18 However, many "highperformance" polymers are synthesized using organometallic reagents, such as stannyl-functionalized monomers for Stille cross-coupling polymerizations, that create stoichiometric amounts of toxic waste and leave residual metals in the final polymer. This has motivated researchers to develop direct arylation polymerization (DArP) protocols to attain structurally diverse conjugated polymers. 19-22 However, while there has been significant diversification of monomers amenable to DArP protocols, incorporating the resulting polymers into efficient devices (such as OPVs) is less prevalent.²³ As such, there is a need to continue to explore monomers amenable to DArP that create "synthetically simple" D-A copolymers while also elucidating the resulting structure-property-performance relationships.

1,4-Dihydropyrrolo[3,2-b]pyrroles (DHPPs) represent a class of organic chromophores with expansive tailorability that is accompanied by simple synthetic and purification protocols.²⁴ These attributes have led to these materials receiving significant attention over the last decade. Research involving DHPPs was catalyzed after the Gryko group demonstrated their ability to be synthesized in a single aerobic step from anilines and aldehydes.²⁵ Over the years, this simple synthesis of DHPPs has enabled access to a diverse family of chromophores with properties such as aggregation-induced emission, ^{26,27} two-photon absorbance/fluorescence, ^{28–32} and molecular resistive memory.33 There also are examples of molecular D-A DHPPs being synthesized and incorporated into optoelectronic devices. 34-36 For example, DHPPs functionalized with dicyanovinylenes have been used as the lightharvesting material in solution-processable bulk heterojunction OPVs while DHPPs containing carbazole or thienyl moieties have been used in dye-sensitized solar cells (DSSCs). Furthermore, a benzothiadiazole-functionalized DHPP was shown to exhibit an external quantum efficiency (EQE) of 3.4% when used as the emissive layer in an OLED device.

These preliminary successes of molecular systems motivate studying D-A DHPPs in polymeric materials.

Recently our group reported the first examples of DHPP comonomers being directly incorporated into the main chain of a polymer repeat unit via DArP³⁷ or acid-catalyzed polycondensation.³⁸ The polymer coupled with a dioxythiophene comonomer (that we abbreviated DHPP-co-ProDOT) exhibited multi-colored electrochromism, led to a quantifiable reduction in the synthetic complexity compared to other conjugated polymers, and delocalized electron density in density-functional theory (DFT) calculations. These attributes and applicability, combined with the simple synthesis and purification, make DHPP a promising candidate as a tailorable monomer to simplify the synthetic complexity commonly associated with D–A copolymers.

Herein, we describe the first examples of DHPP-based D-A copolymers synthesized via DArP with thieno[3,2-b] pyrrole-4,6-dione (TPD) and 3,6-bis(2-thienyl)-2,5-dihydropyrrolo[3,4-c]pyrrole-1,4-dione (Th₂DPP) as the electrondeficient comonomers. The synthetic complexity was quantified to reveal that DHPP-based D-A polymers reduce the synthetic complexity by ~35% compared to polymers synthesized with TPD and Th₂DPP comonomers and are amongst the simplest D-A copolymers synthesized via DArP. Initial understanding of structure-property relationships of these novel D-A polymers are understood by investigating how monomer structures influence synthetic accessibility as well as optical, electrochemical, and thermal properties. Furthermore, we investigate the functionality of these polymers as active layer materials in redox and solidstate applications by studying their electrochromic properties and using them as light-absorbing polymers in bulk heterojunction (BHJ) solar cells. Notably, the polymer DHPP-alt-Th2DPP exhibits colored-to-transmissive electrochromism and an average PCE of 2.5% in BHJ OPVs. Combined, this study reinforces the notion that DHPP offers a readily accessible and tunable scaffold for incorporation into D-A design paradigms while simultaneously demonstrating the expanded functionality of these underutilized materials.

2 | RESULTS AND DISCUSSION

The solubility of dihydropyrrolephrole-based polymers has proven to be an impediment to isolation, purification, and thorough solution characterization. As such, and as shown in Scheme 1, we used a two-step process starting with the alkylation of acetaminophen followed by deprotection via hydrolysis of the acetyl group to introduce side chains hypothesized to facilitate solubility in organic solvents. Column chromatography was omitted from the intermediate synthetic step since the inherent solubility differences at

SCHEME 1 Overall synthetic scheme for synthesizing tailorable organic soluble DHPP monomers through (A) the alkylation and deprotection of acetaminophen followed by (B) the Fe(III)-catalyzed multicomponent reaction.

(A)

Br-R

KI

K₂CO₃

2-Butanone

Reflux

OR

$$R = -(2-\text{EthylHexyl}) \text{ Yield: } 98\% \\ -(2-\text{HexylDecyl}) \text{ 86\%}$$

R= -(2-EthylHexyl) Yield: 56%

-(2-HexylDecyl) 64%

(B)

$$R = -(2-\text{EthylHexyl}) \text{ Yield: } 37\% \\ -(2-\text{HexylDecyl}) \text{ 47\%}$$

room temperature between alkyl-functionalized anilines and 4-aminophenol allowed for relatively easy separation during liquid-liquid extraction. TLC showed no 4-aminophenol remained in the organic phase after extraction of functionalized anilines. With this pathway, 4-(2-(ethylhexyloxy)) aniline and 4-(2-(hexyldecyloxy))aniline (EtHx-HxDec-aniline, respectively) were successfully synthesized and verified via NMR (Figures S1-S4). The two alkyloxyanilines were subsequently used in the Fe(III)-catalyzed multicomponent reaction³⁹ with 4-bromobenzaldehyde to generate the 2,5-bis(4-bromophenyl)DHPP monomers where the 4-positions of the 1,4-bis(phenyl) units were functionalized with ethylhexyloxy- or hexyldecyloxygroups. The solids that precipitated from the reaction mixture were collected via vacuum filtration and purified by washing with cold methanol and acetone to produce monomers EtHxDHPP and HxDecDHPP with yields of 37% and 47%, respectively. ¹H, ¹³C NMR, and elemental analysis were used to confirm the structure and purity of the monomers (Figures S5–S8). Specifically, the singlet \sim 6.4 ppm for both monomers is diagnostic for DHPPs and the close agreement between theoretical and experimental elemental analysis values supports the notion that monomers are of adequate purity for polymerization.

TPD and Th_2DPP represent promising electrondeficient comonomers for polymerization with DHPP to access D–A copolymers. This stems from these comonomers being successfully incorporated into D–A copolymers via DArP and has been studied for many organic applications,

including OPVs and OLEDs. 40,41 Initial efforts involved functionalizing Th2DPP with 2-ethylhexyl (EtHx-) or 2-octyldodecyl (OcDo-) alkyl chains followed by polymerization with DecylDHPP, 37,42 EtHxDHPP, or HxDecDHPP using the anhydrous DArP conditions as illustrated in Scheme 2 and reported in Table 1. As listed in Table 1, Entry 1 yielded mostly insoluble material meaning EtHx solubilizing chains solely on the Th₂DPP are insufficient for attaining a soluble DHPP-alt-Th₂DPP copolymer. Entry 2 involved using EtHx chains on both comonomers and vielded identical proportions of insoluble materials to Entry 1 indicating larger branched side chains are required. Entry 3 and 4 used OcDo side chains on the Th₂DPP monomer and Dec or HxDec functionalities on DHPP, which yielded soluble fractions in 32% and 96%, respectively. However, their number-average molecular weights (M_n) were unsatisfactory for observing electronic properties independent of molecular weight and inspired further screening of polymerization conditions.

The DArP conditions were finally optimized by replacing toluene with cyclopentyl methyl ether (CMPE), a green solvent derived from biomass, 43,44 and performing the reaction in a pressure vessel. The optimized conditions (Table 1, Entry 5) yielded a dark blue polymer in 96% yield with a $M_{\rm n}$ of 30.5 kg/mol vs polystyrene standards, and a dispersity ($D=M_{\rm w}/M_{\rm n}$) of 2.5 as determined via SEC. As shown in Figure S16a, the SEC elugram exhibits a monomodal molecular weight distribution indicating that the previous solubility limitation has been

$$\begin{array}{c} RO \\ Br \end{array} + \begin{array}{c} R' \\ S \\ N \\ N \end{array} \\ \begin{array}{c} Catalyst \\ PCy_3 \cdot HBF_4 \\ \hline Cs_2CO_3 \\ Solvent \\ Temperature \end{array} \\ \begin{array}{c} R' \\ OR \end{array} \\ \begin{array}{c} R' \\ N \\ N \\ OR \end{array}$$

R= Decyl-, EthylHexyl-, or HexylDecyl- R'=EthylHexyl- or OctylDodecyl-

SCHEME 2 General DArP polymerization for synthesizing DHPP-alt-Th₂DPP polymers. Results for specific conditions are listed in Table 1.

TABLE 1 Overview of synthetic efforts for developing organic-solvent soluble DHPP-alt-Th₂DPP polymers.

	•						
Entry	DHPP side chain	Th ₂ DPP side chain	Pd source/ ligand	Solvent/temp (°C)	Soluble yield (%)	M _n (kg/mol)	$\theta (M_{\rm w}/M_{\rm n})$
1	$-C_{10}H_{21}$	—EtHx	$Pd(OAc)_2$	Toluene	11	_b	_b
			PCy₃·HBF₄	110			
2 ^a	—OEtHx	—EtHx	$Pd(OAc)_2$	Toluene	12	_b	_b
			PCy₃·HBF₄	130			
3 ^a	$-C_{10}H_{21}$	—OcDo	$Pd(OAc)_2$	Toluene	32	2.3	1.3
			PCy₃·HBF₄	130			
4 ^a	—OHxDec	—OcDo	Pd ₂ (dba) ₃	Toluene	96	8.6	1.8
			PCy₃·HBF₄	130			
5 ^a	—OHxDec	—ОсDо	$Pd(OAc)_2$	СРМЕ	96	30.5	2.5
			$PCy_3 \cdot HBF_4$	130			

^aThese reactions were performed in a pressure vessel.

overcome while maintaining a controlled polymerization. Due to the limited solubility of final HxDecDHPP-alt-OcDoTh₂DPP (Entry 5) in CDCl₃, its lower molecular weight analog was used for NMR analysis to verify the successful connectivity of monomers as an alternating copolymer (Figure S13). The resulting polymer retains the pyrrolic hydrogen located at 6.38 ppm and the hydrogens corresponding to the thienyl protons of the Th₂DPP comonomer at 7.29 ppm were converted from triplets to doublets (see Figures S7, S9, and S10). A closer analysis of the aromatic region of the ¹H NMR spectrum reveals the absence of defects within the final polymer. This is determined by comparing integration values of peaks associated with the pyrrolic protons and thienyl protons immediately adjacent to the Th₂DPP monomer unit. As shown in Figure S14, the peaks integrate to a nearly perfect 1:1 ratio which supports our notion of high compositional purity. Purity and composition were further verified with elemental analysis that

showed similar values for expected and determined elemental compositions. In total, these results confirm the first successful synthesis of a DHPP-containing D-A copolymer. This polymer will be abbreviated as DHPP-alt-Th₂DPP for simplicity throughout the remainder of the manuscript.

After the successful polymerization of DHPP with ${\rm Th_2DPP}$, we turned to incorporating DHPP into a polymer with TPD as the comonomer. TPD was synthesized using a direct imide formation reaction⁴⁵ and subsequently alkylated with 9-(bromomethyl)nonadecane to yield 2-octyldodecyl-TPD (OcDoTPD), as described in Scheme 3A. As shown in Scheme 3B, using the optimized anhydrous DArP condition developed for DHPP-alt-Th₂DPP, HxDecDHPP-alt-OcDoTPD was successfully synthesized with a 99% yield, a $M_{\rm n}$ of 74.6 kg/mol, and D=3.0 as determined by GPC (see Figure S16b). The GPC trace for this polymer also shows a monomodal molecular weight distribution, demonstrating the

^bThe resulting products did not possess adequate solubilities in solvents used in SEC measurements.

SCHEME 3 (A) Synthetic pathway to produce OcDoTPD and (B) synthesis of DHPP-alt-TPD using optimized anhydrous DArP conditions.

solubility constraints previously described have been overcome. Structure, purity, and composition were further verified using ¹H NMR (Figure S15) and elemental analysis indicating a successful synthesis of HxDecDHPP-alt-OcDoTPD. For convenience, this polymer will be abbreviated DHPP-alt-TPD.

One of the overarching goals of this project is to simplify the synthesis of D-A conjugated polymers. Po et al. developed Equation 1 to quantify the synthetic complexity (SC) for the syntheses of conjugated polymers. This study benchmarked numerous D-A polymers (>100) and provides several systems for comparing the DHPPcontaining copolymers to the field. As shown in entries 1 and 2 in Table 2, the average SC for D-A polymers synthesized with Th₂DPP and TPD comonomers is 40.6 and 45.4, respectively. Contrastingly, the synthetic complexities of DHPP-alt-Th2DPP (entry 3) and DHPP-alt-TPD (entry 4) are 25.3 and 28.9, respectively. It is evident from Table 2 that the most significant contributors to the reduction in the synthetic complexity of our DHPP D-A copolymers are the minimization of synthetic steps (NSS), number of operations required for purification of monomers (NUO), and use of hazardous materials (NHC). Overall, the synthetic complexity of

Th₂DPP- and TPD-containing D-A copolymers is reduced by ~37% when copolymerized with DHPP comonomers which supports the notion that continued investigation into structure-property relationships of DHPP-containing copolymers is warranted. Turning to compare the synthetic complexity of DHPP-alt-Th₂DPP and DHPP-alt-TPD to polymers synthesized via DArP that have also demonstrated respectable device properties in OPVs (entries 5-14) or high-contrast electrochromes (entries 15-17), DHPP-alt-Th₂DPP and DHPPalt-TPD are more simple when compared to \sim 60% of the polymers listed in Table 2. Structures corresponding to these polymers are collected in Figure S17. Once again the number of synthetic steps is a major factor determining the synthetic complexity of the resulting polymers. Specifically, polymers that are attained with a lower number of synthetic steps result in lower synthetic complexity. Another notable attribute of DHPPcontaining polymers is the reduction of using hazardous compounds (NHC) compared to many of the polymers listed in Table 2. Combined, we have demonstrated DHPP as a viable monomer to simplify the synthesis of D-A conjugated polymers while using concepts of green chemistry.

TABLE 2 Synthetic complexity analysis of D-A copolymers and comparison to DHPP-containing copolymers.

Entry	Polymer ^a	NSS	RY	NUO	NCC	NHC	SC	Ref. ^b
1 ^c	Th ₂ DPP copolymer avg.	8.6 (±2.9)	9.6 (±6.3)	15.1 (±6.1)	3.6 (±1.6)	22.2 (±10.1)	40.6 (±11.7)	[6]
2 ^c	TPD copolymer avg.	9.8 (±1.3)	12.7 (±19.5)	18.1 (±3.2)	4.5 (±2.8)	25.6 (±6.0)	45.4 (±11.6)	[6]
3	DHPP-alt-Th ₂ DPP	6	8.2	2	1	9	25.3	This Work
4	DHPP-alt-TPD	6	19.0	1	1	6	28.9	This Work
5	P3HT	3	1.1	4	0	4	7.75	[6]
6	PEDOTF	4	2.3	7	1	10	17.1	[46]
7	PDCBT	3	1.8	5	2	8	14.1	[47]
8	PM6	12	19.9	22	8	31	60.57	[48]
9	PBDTT-FTTE	14	10.5	22	8	28	59.5	[49]
10	DTBDT-alt-BTz	8	19.3	16	6	21	47.2	[50,51]
11	PDFBT-Th ₄	8	5.9	13	3	15	34.5	[52]
12	PBDB-T	10	8.6	17	4	34	46.8	[48]
13	PPDT2FBT	8	7.8	14	4	32	41.5	[53]
14	P3	7	6.2	12	2	13	31.3	[54]
15	ECP-Blue	3	1.4	2	2	6	11.1	[55]
16	ECP-Cyan	4	1.9	3	4	9	17.6	[55]
17	ECP-Black	6	4.1	5	5	11	27.7	[55]

^aFor a comprehensive tabulation of synthetic complexity for conjugated polymers, readers are directed to the work described in Ref. [6].

$$\begin{split} SC = 35 \frac{\text{NSS}}{\text{NSS}_{\text{max}}} + 25 \frac{\log(\text{RY})}{\log(\text{RY}_{\text{max}})} + 15 \frac{\text{NUO}}{\text{NUO}_{\text{max}}} \\ + 15 \frac{\text{NCC}}{\text{NCC}_{\text{max}}} + 10 \frac{\text{NHC}}{\text{NHC}_{\text{max}}} \end{split} \tag{1}$$

The use of conjugated polymers in optoelectronic devices, such as OPVs, motivated our investigations into the light-absorbing properties of DHPP-based D-A polymers using UV-vis absorbance spectroscopy. As shown in Figure 1A, the DHPP-alt-Th₂DPP polymer exhibits a dualband absorbance profile. The high energy (~380 nm) and low energy maxima (\sim 550 < λ < 750 nm) are attributed to π - π * and intramolecular charge transfer (ICT)^{14,15} transitions, respectively. As the molecular weight increases from Entry 1 to Entry 5, the low energy band exhibits a broadening phenomenon, the evolution of vibronic features (to greater or lesser extents), and a noticeable red shift in their respective λ_{max}^{abs} and absorbance onset. It should be noted that a similar but significantly smaller occurrence can be seen in the high energy band even though it exhibits less dependence on polymer molecular weight. When comparing Entry 4 and 5, both traces exhibit similar high energy absorbance bands with a λ_{max}^{abs} \sim 384 nm. Where these two differ is in the low energy ICT band, with Entry 5 exhibiting a broad absorbance band with

absorbance features consistent with the largest extent of vibronic structure that is minimized for its lower molecular weight counterparts. This vibronic structure is attributed to the higher molecular weight achieved and can be indicative of a higher degree of aggregation between polymer chains. 16,17 Temperature-dependent UV-vis absorbance spectroscopy was used to investigate this phenomenon, and as shown in Figure 1B, Entry 5 exhibits temperature-dependent absorbance in dilute solutions based on changes in the absorbance spectra with increasing temperature. Specifically, the polymer exhibits thermochromic behaviors that shift from displaying vibronic features to a more uniformed band with increasing temperature. The absorbance shifts from $\lambda_{max}^{abs} \approx 725 \, nm$ at 25°C to 646 nm at 100°C, indicating that the polymer aggregates are disrupted in addition to conformational changes of non-aggregated species^{56–58} and the polymer is better solubilized.⁵⁹ This same polymer is also solution processable and shows more defined vibronic features in the absorbance spectrum as a film compared to the solution (Figure 1C). Combined, these changes further emphasize the importance of synthetic conditions, monomer purity, and solubilizing functionalities when designing conjugated polymers.

As shown in Figure 1D, DHPP-alt-TPD exhibits a single absorbance band when dissolved in toluene (\sim 30 μ g/mL)

^bReference(s) used for tabulation of synthetic complexity.

^cAverages are calculated from synthetic complexity data compiled and reported in Ref. [6]. Calculated values are representative of 18 Th₂DPP- and 9 TPD-containing copolymers.

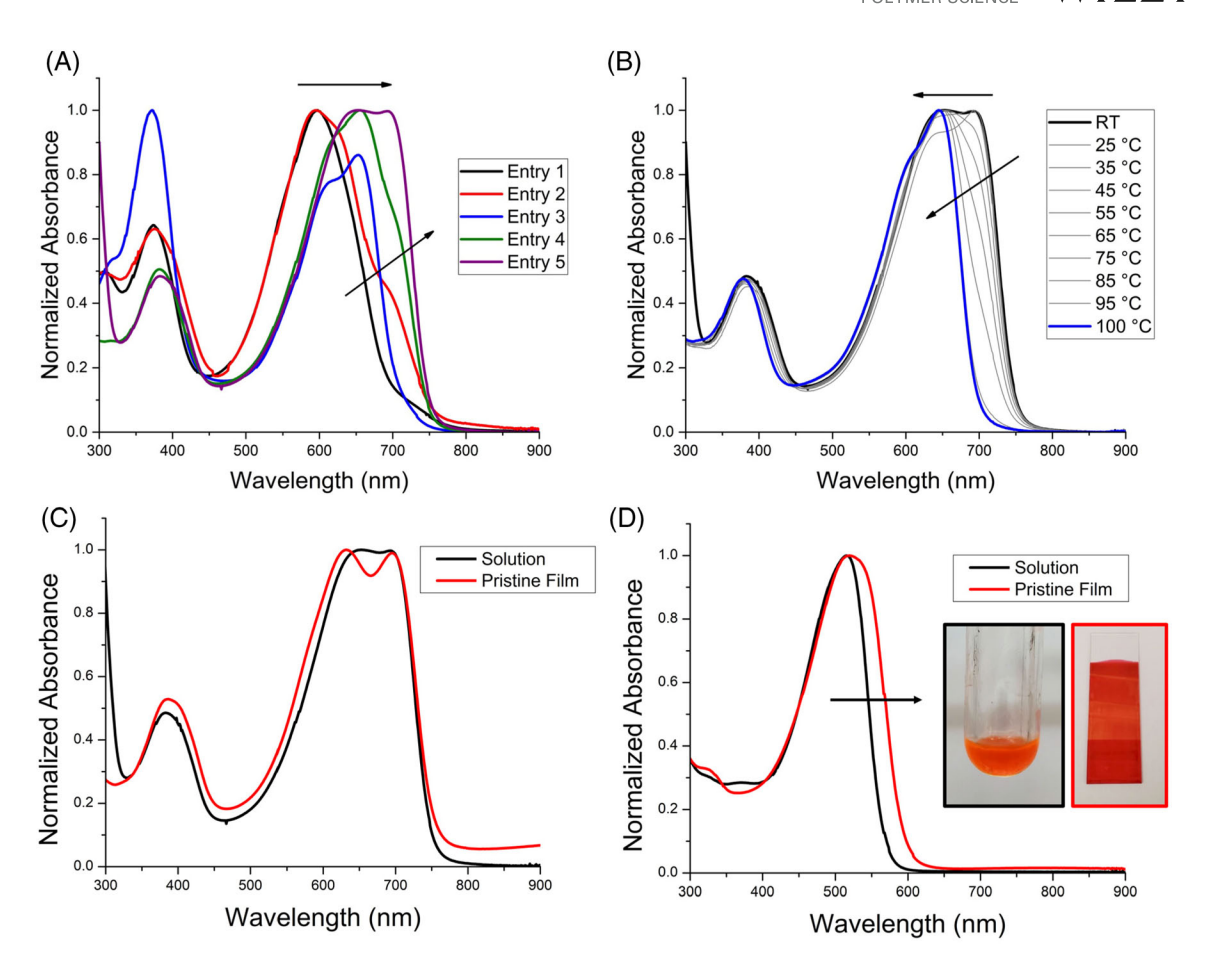


FIGURE 1 (A) Solution absorbance spectra of DHPP-alt-Th₂DPP in dilute toluene solutions showing the evolution of DHPP-alt-Th₂DPP as a function of the M_n . (B) Temperature-dependent absorbance spectra of DHPP-alt-Th₂DPP in toluene heating from RT to 100 °C. (C) UV-vis absorbance spectra of DHPP-alt-Th₂DPP in solution (black) with a nominal concentration of \sim 10 μ g/mL and a spray-coated polymer film (red). (D) UV-vis absorbance spectra of DHPP-alt-TPD in solution (black) with a nominal concentration of \sim 50 μ g/mL and a manually blade-coated polymer film (red). Pictures in the inset show the polymer solution and deposited film and are presented without manipulation.

with a λ_{max}^{abs} of 516 nm likely corresponds to an ICT transition while the "basic" π - π * transition occurs below 300 nm and outside the experimental range. This assumption is supported by calculations of DHPP-TPD oligomers that predict a dual-band absorbance profile where the high energy transition resides ~300 nm. 37 DHPP-alt-TPD also emits a vibrant orange color when irradiated with UV light. Since conjugated polymers are commonly processed as thin films for organic electronic devices, we were motivated to investigate this polymers' processability and properties when cast as a thin film. We successfully deposited a thin film via blade coating using $a \sim 20 \text{ mg/mL}$ toluene solution of DHPP-alt-TPD which is desirable for scalable film production.⁶⁰ As the solvent evaporated and the polymer transitioned from solution to the solid state the perceived color of the polymer changed from an orange-red color in solution to a vibrant red as a thin film. This film, as well as the film measured to create Figure 1C, is likely \sim 300–350 nm thick. This inference is

based on work reported by Padilla and coworkers that examined electrochromic performance based on the deposition method and found that many polymers processed using spray coating and blade coating regularly produced films around this thickness.⁶¹ As a thin film, DHPP-alt-TPD exhibited a slightly red-shifted absorbance compared to solution absorbance resulting in a λ_{max}^{abs} of 519 nm, a lower absorbance onset, and a broader absorbance profile. This absorbance broadening can be attributed to increased π - π interactions between polymer chains as well as an increased planarization of the polymer backbone in the solid state compared to a fully solvated polymer. Optoelectronic properties associated with both polymers is tabulated and reported in Table 3. Combined, these findings reveal the feasibility of manufacturing thin films with DHPP-based D-A polymers using processing methods desired for large-scale production that will be useful for their incorporation into organic electronics, such as OPVs, OLEDs, or electrochromics.

TABLE 3 Optoelectronic properties of DHPP-containing donor-acceptor copolymers.

Polymer	$\lambda_{\max}^{\mathrm{sol}}(\mathbf{nm})$	$\lambda_{\max}^{\text{film}}(\mathbf{nm})$	HOMO (eV)	LUMO (eV)	$E_{\rm gap}$ (eV)	$\boldsymbol{E}_{\mathrm{onset}}^{\mathrm{ox}}$ (V)	$\mu_{\rm h}~({\rm cm^2V^{-1}~s^{-1}})$
DHPP-alt-Th ₂ DPP	725	725	-5.53	-3.90	1.63	0.80	3.26×10^{-4}
DHPP-alt-TPD	516	519	-5.66	-3.66	2.00	0.95	4.34×10^{-6}

Thermal properties of D-A DHPP-based polymers, including degradation temperature (T_d) , glass transition (T_g) , and crystallization temperature (T_c) , were investigated using thermal gravimetric analysis (TGA) and differential scanning calorimetry (DSC), respectively. TGA was used to determine the degradation temperature of these polymers by measuring the mass loss as a function of temperature. Figure \$18a shows the TGA traces that indicate DHPP-alt-Th2DPP and DHPP-alt-TPD have degradation temperatures of 370 °C and 339 °C, respectively. TGA also gives insight, and supports our NMR and elemental analysis results, to the purity of the resulting polymers evident by the level trace from r.t. to \sim 300 °C. DSC measurements show no thermal transitions (T_g or T_c) within the experimental range revealing that these polymers are amorphous as bulk samples (Figure S18b). The lack of an observable $T_{\rm g}$ has been attributed to the backbone rigidity of conjugated polymers. 62 The high thermal stability of these polymers makes them amendable to post-processing annealing protocols commonly used for the preparation of organic electronics, further motivating the continued study of this novel class of conjugated polymers into organic electronic devices.

Differential pulse voltammetry (DPV) was used to accurately measure the oxidation onsets that are used to estimate ionization energies (IE) of DHPP-alt-Th₂DPP and DHPP-alt-TPD. Measurements were taken of fresh films for each electrochemical sweep and the onsets of oxidation (E_{onset}^{ox}) were extracted from the first DPV sweep. These precautions eliminate any chemical or morphological alterations that may arise due to the flux of ions and solvents through the film with repeated electrochemical cycling. 63,64 As shown in Figure S20, both polymers display relatively low onsets of oxidation. Specifically, DHPP-alt-Th₂DPP (Figure S20a) exhibits an $E_{\text{onset}}^{\text{ox}}$ of 0.41 V versus the ferrocene/ferrocenium (Fc/Fc⁺) redox couple with the main oxidation $\sim 0.7 \, \text{V}$. DHPP-alt-TPD displays a small electrochemical response that is measured with an onset ~0.44 V versus Fc/Fc⁺ and a second more pronounced oxidation beginning ~0.7 V. The IE (i.e., HOMO) for each polymer is subsequently calculated using the equation $E_{\rm IE} = -e(E_{\rm onset}^{\rm ox} + 5.12)$ where the energy level of Fc/Fc⁺ versus vacuum is assumed to be -5.12 eV.⁶⁵ Using this approach, DHPP-alt-Th₂DPP possesses an estimated HOMO level of -5.53 eV. The lowest unoccupied orbital (LUMO) of DHPP-alt-Th2DPP is

calculated to be $-3.90\,\mathrm{eV}$ after determining the optical bandgap (E_g) from the onset of absorbance (\sim 760 nm). The HOMO and LUMO energy levels for DHPP-alt-TPD are calculated to be $-5.66\,\mathrm{and}$ $-3.66\,\mathrm{eV}$, respectively. Importantly, both polymers possess appropriate energy-level alignments with the electron acceptor PCBM⁶⁶ which makes them suitable as electron-donating material in bulk heterojunction blends used as the active layer for OPVs.

Next, the redox properties of the D-A polymers as thin films were studied via cyclic voltammetry (CV). Films were prepared by spray coating polymer solutions onto indium tin oxide (ITO) electrodes and redox potentials of the films were measured in a 0.5 M tetrabutylammonium hexafluorophosphate/propylene carbonate (TBAPF₆/PC) supporting electrolyte solution versus a Ag/AgCl reference electrode. As shown in Figure 2A, DHPP-alt-Th₂DPP shows a distinct onset of oxidation ~0.8 V versus Ag/AgCl as a pristine film and two oxidation and reduction processes. The films were then subjected to electrochemical conditioning processes which consist of 10 CV cycles across a voltage window of -0.5 to 1.2 V versus Ag/AgCl. After conditioning, the CV trace evolves from displaying a sharp onset of oxidation to demonstrating more capacitive-type behavior upon electrochemical conditioning. The CV experiments for DHPP-alt-TPD yielded drastically different results. First, as a pristine film, DHPP-alt-TPD displayed an onset of oxidation \sim 0.6 V versus Ag/AgCl. Second, as shown in Figure 2B, the redox response rapidly diminished during attempts to electrochemically condition films. This was evident from the rapid depletion in the current density within 5 CV cycles. Since there was no change in the color of the electrolyte solution, we attribute this depletion to electrochemical degradation upon the generation of the oxidized species or the evolution of an irreversible redox-inactive species.

Changes in absorbance as a function of electrochemical potential from 0.5–1.2 V versus Ag/AgCl were first evaluated for DHPP-alt-Th₂DPP films processed onto ITO electrodes from 1 mg/mL toluene solutions. As shown in Figure 3A, DHPP-alt-Th₂DPP displays similar vibronic features observed from solution UV-vis absorbance measurements, indicating the aggregated structures are maintained after the film fabrication process and highlighting the importance of aggregated structures and controlling the thin film microstructure.⁶⁷ The absorbance features in the low energy transition are more

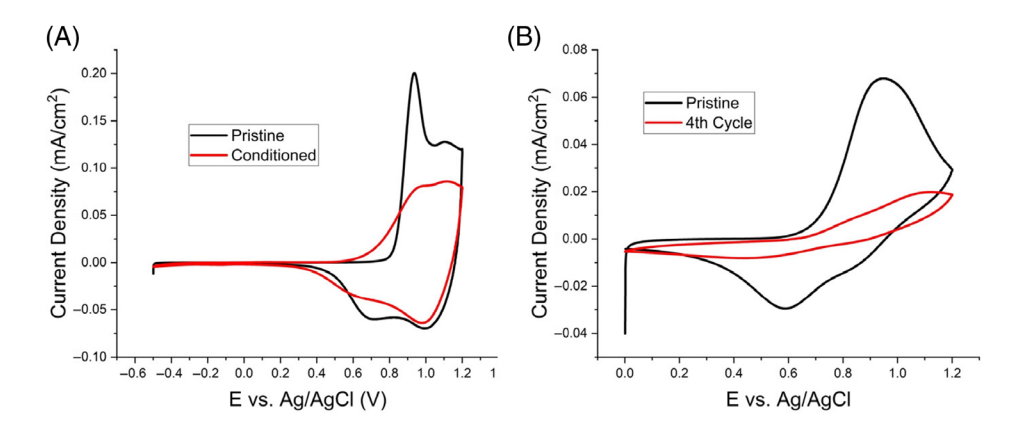
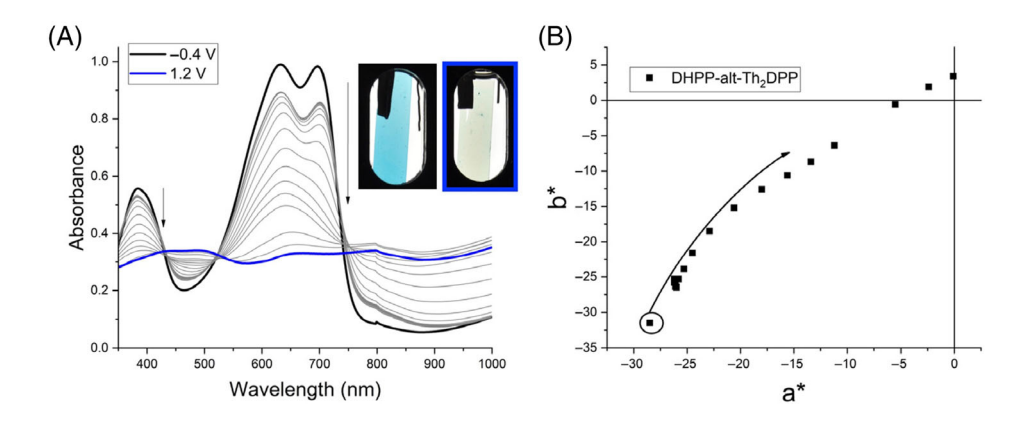


FIGURE 2 Cyclic voltammogram traces of (A) DHPP-alt-Th₂DPP and (B) DHPP-alt-TPD as pristine (black) and electrochemically conditioned films (red). Electrochemical conditioning protocols consist of performing 10 CV cycles across a voltage window of -0.5 to 1.2 V for DHPP-alt-Th₂DPP and 0.0 to 1.2 V for DHPP-alt-TPD (vs. Ag/AgCl reference electrode, $E_{1/2} = 46$ mV vs. Fc/Fc⁺) in 0.5 M TBAPF₆/PC electrolyte solution using a scan rate of 50 mV/s.

FIGURE 3 (A) Absorbance spectra as a function of applied potential and photographs of a DHPP-alt-Th₂DPP film spray cast from a 1 mg/mL toluene solution by applying 50 mV potential intervals from -0.5 V to 1.2 V in 0.5 M TBAPF₆/PC supporting electrolyte and; (B) color coordinates of a DHPP-alt-Th₂DPP film spray cast from toluene as a function of applied potential.



defined as a processed film indicating a slight increase in intrachain interactions brought on by an increase in order. As the electrochemical potential is increased, the absorbance begins to diminish at $\sim 0.6 \, \text{V}$ versus Ag/AgCl, which corresponds well with the onset of oxidation. As the electrochemical potential is increased to 1.2 V versus Ag/AgCl, the absorbance continues to diminish which indicates the polymer transitions from a colored, neutral state to a transmissive film when oxidized. This phenomenon is depicted by the photographs in the inset of Figure 3A that show DHPP-alt-Th₂DPP as a cyan neutral film and a transmissive oxidized film and highlights the potential of using this polymer as a highcontrast electrochrome. Alternatively, DHPP-alt-TPD is a vibrant pink-red color as a neutral film that transitions to a dull, brown-orange color (Figure S20). This color change is not reversible and, since the film does not delaminate, we attribute these changes to the formation of a new electroactive species that is electrochemically irreversible. This notion is further supported by the diminished electrochemical response observed in CV experiments (Figure 2B).

Colorimetric analysis of DHPP-alt-Th₂DPP polymer films based on the "Commission Internationale de l'Eclairage" 1976 $L^*a^*b^*$ color standards was used to quantify the observed color change during spectroelectrochemical experiments. Colorimetry data in Figure 3B indicates DHPP-alt-Th2DPP lies in the color quadrant between the blue $(-a^*)$ and green color $(-b^*)$ space. As a conditioned, neutral film, DHPP-alt-Th₂DPP possesses a^* and b^* values ~ -25 and agrees with the measured UV-vis absorbance spectrum and the cyan color shown in the photographs in Figure 3A. The cyan color derives from the dual-band absorbance profile with a transmissive window between 450 and 500 nm in addition to the high-energy transition appearing mostly in the UV portion of the electromagnetic spectrum and the charge-transfer transition possessing an absorbance onset of \sim 760 nm. ^{68–70} As the electrochemical potential is increased with continued 50 mV steps, the absorbance begins to diminish and the resulting color coordinates track towards the graph's origin. This track ultimately reveals the oxidized polymer to display small a^* and b^* values (-0.1 and 3.4, respectively) as well as an L^* value of \sim 75. Combined with the photograph in the inset

of Figure 3A, these results indicate that DHPP-alt-Th2DPP can attain a transmissive, color-neutral oxidized state and supports the potential utility in color-to-transmissive electrochromic applications. DHPP-based molecules have been studied in BHJ OPV applications, which motivated our investigation into determining the viability of DHPP D-A copolymers as active layer material in OPV devices. DHPP copolymers (CPs) were blended in chlorobenzene solutions with a 1:1.2 ratio with [6,6]-phenyl-C71-butyric acid methyl ester (PC₇₁BM) as the electron-acceptor phase material and 2% diiodooctane. Blends were stirred at 100 °C for 2 h before deposition onto patterned ITO electrodes via spin-coating. Preliminary devices with device architectures of ITO/zinc oxide/CP:PC71BM/molybdenum oxide/silver were constructed and used to measure OPV device performance. The average device parameters from 6 devices and current density-voltage (J-V) curves of the best-performing devices are reported in Figure 4 and Table 4. First, both DHPP-alt-Th₂DPP and DHPP-alt-TPD display a photovoltaic response, evident by calculating average PCEs of 2.5 ± 0.22 and 1.1 ± 0.07 , respectively. The key difference in PCEs is attributed to the significant enhancement of the short-circuit current density (J_{sc}) for DHPP-alt-Th₂DPP (8.7 \pm 0.76 mA cm⁻²) compared to the $J_{\rm sc}$ measured for DHPP-alt-TPD (3.1 ± 0.20 mA cm⁻²) while other factors such as morphology, energy level alignment, surface and bulk traps may also play a role.⁷¹ For example, as shown in Figure S21, a high concentration of what are believed to be PCBM aggregates/crystallites are present across multiple length scales in a DHPP-alt-Th₂DPP/PC₇₁BM film processed using the same conditions to construct devices. It is well established that the size and morphology of fullerene aggregates directly influence device performance and the presence of these features likely diminishes efficient charge transport needed for high-efficiency devices. 72,73 The increased J_{sc} for DHPPalt-Th2DPP compared to DHPP-alt-TPD is attributed to DHPP-alt-Th2DPP absorbing a larger fraction of photons

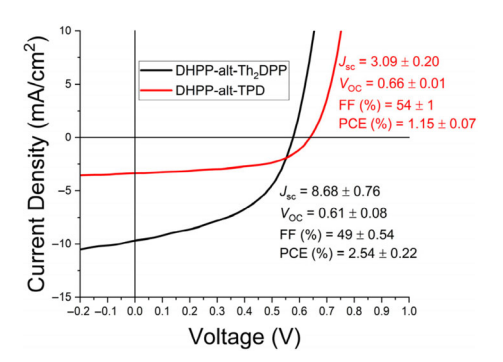


FIGURE 4 Solar cell *J-V* curves for polymer/PC₇₁BM devices using DHPP-alt-Th₂DPP (black) and DHPP-alt-TPD (red) as the electron-donor material.

irradiated from the solar spectrum.⁷⁴ While it is not unexpected that results from these unoptimized devices do not meet or surpass PCEs of D–A copolymers synthesized with analogous electron-deficient monomers,^{75–77} these preliminary results show improved device performance compared to molecular DHPP chromophores³⁴ and provide precedent to continue exploring DHPP-containing D–A copolymers as active layer materials in OPVs. It is worth noting there are a variety of optimization strategies that may result in improved PCE values. Strategies that use solvent or non-volatile solid additives,^{78,79} thermal or solvent vapor annealing,⁸⁰ or alternative film fabrication methods, including electrospinning⁸¹ or blade coating,⁸² have all yielded higher PCE values and may be useful for future studies.

Nonfullerene acceptors (NFAs) are a relatively new class of acceptor material that has led to significant improvement in device performance efficiencies when blended with donor material.83 Here, we sought to improve the device performance by blending the DHPPbased D-A polymers with the NFA Y12. The structure of Y12 and details for assembling hole-only devices are included in the Supporting Information and results are summarized in Table 4. As shown in Figure S22, PCEs remained at ~2.4% for DHPP-alt-Th₂DPP and dropped to \sim 0.54% for DHPP-alt-TPD. The higher PCE for DHPP-alt-Th₂DPP in both blend compositions infers that the limiting factor for improving PCEs is the charge carrier mobilities of the materials. This inference motivated measuring charge mobility (μ) with space-chargelimited-current (SCLC) measurements. As shown in Figure S23, our initial reasoning was confirmed by DHPPalt-Th2DPP having 2 orders of magnitude larger average mobility ($\mu_{\rm avg}$) than DHPP-alt-TPD ($\mu_{\rm avg}=3.26\times 10^{-4}$ $cm^2V^{-1}s^{-1}$ vs. 4.34×10^{-6} $cm^2V^{-1}s^{-1}$, respectively). Notably, the measured mobilities here represent 3-5 orders of magnitude increase compared to molecular DHPPs that have been studied in bulk heterojunction devices.³⁴ The increase in mobilities for polymers compared to molecular systems alludes to a molecular weight dependence on device performance and serves as a future avenue of study for elucidating DHPP structure-property relationships. Importantly, the out-of-plane hole mobility of these polymers is in the range of many high-performing and successfully developed materials in BHJ OPVs. For example, Blom et al. have shown that the best device efficiencies are achieved in the mobility range of 10^{-6} – 10^{-4} cm²V⁻¹ s⁻¹ in their model developed for PCBM-based solar cells.84 Moreover, the recent OPV benchmark system of PM6:Y6 (structures shown in Figure S24) with the reported performance of PCEs of 15%-17% is measured to have hole mobility of 0.21×10^{-4} – 0.7×10^{-4} $cm^2V^{-1}s^{-1.85,86}$

TABLE 4 Photovoltaic parameters of the polymer/Y12 OPV devices measured under AM 1.5G illumination.

System	$J_{ m SC}$ (mA cm $^{-2}$)	$V_{ m OC}$ (V)	FF (%)	PCE (%) (best)	Thickness (nm)
DHPP-alt-TPD: PC ₇₁ BM	3.09 ± 0.20	0.66 ± 0.01	54 ± 1.0	$1.15 \pm 0.07 (1.25)$	100 ± 10
DHPP-alt-Th ₂ DPP: PC ₇₁ BM	8.68 ± 0.76	0.61 ± 0.08	49 ± 0.54	2.54 ± 0.22 (2.85)	160 ± 10
DHPP-alt-TPD:Y12	2.61 ± 0.11	0.69 ± 0.001	28.06 ± 1.41	$0.54 \pm 0.04 (0.59)$	150 ± 10
DHPP-alt-Th ₂ DPP:Y12	9.40 ± 0.44	0.52 ± 0.01	47.09 ± 1.47	2.41 ± 0.13 (2.68)	150 ± 10

3 | CONCLUSIONS

Creating new D-A motifs that enable accessing conjugated materials with targeted properties is essential for the continued advancement of organic electronics. Simultaneous simplification of the synthesis of these systems also is desired so that continued improvement in device performance metrics is achieved with sustainable considerations. Specifically, it is necessary to reduce the number of synthetic steps, minimize/simplify purification protocols, and exploit high-yielding polymerizations that eliminate the evolution of toxic byproducts without sacrificing the ability to attain desired properties for specific applications. In this vein, we have demonstrated DHPP-based D-A copolymers to be amongst some of the most synthetically simple D-A copolymers while expanding the knowledge of fundamental structure-property relationships of an underutilized monomeric building block (DHPP). This study reports side-chain engineering strategies that enable DHPP monomers to be incorporated into D-A copolymers with high molecular weights and sufficient solubilities to accurately elucidate foundational structure-property relationships. It is worth noting that both copolymers reported here are synthesized in CPME, a biomass-based renewable solvent, which further reinforces the utility of DHPPs for synthesizing sustainable materials. Investigation of the optical properties of DHPP copolymers constructed with the electron-deficient comonomers Th2DPP and TPD revealed that the resulting copolymers demonstrate narrow optical bandgaps due to the ICT phenomenon from the electron-rich DHPP to the acceptor building block. Additionally, electrochemical studies using DPV and CV revealed that DHPP-alt-Th2DPP and DHPP-alt-TPD possess appropriate energy level alignment to facilitate charge transfer processes necessary to extract photoexcited electrons in bulk heterojunction blends. Both polymers also possess high thermal stability ($T_d \ge 340 \,^{\circ}\text{C}$) which makes them amenable to post-processing annealing protocols commonly used for thin film optoelectronic studies, if required. These DHPP-containing D-A copolymers demonstrate their potential utility as active layer material in organic electronic applications through electrochromic and OPV measurements. Notably, DHPP-alt-Th2DPP

displays colored-to-transmissive electrochromism and a 2.5% average PCE when used in bulk heterojunction OPVs. In sum, the ease of functionalization of DHPPs, their ability to react with donors and acceptors, and their applicability in various optoelectronic applications make them appealing building blocks for organic electronics.

ACKNOWLEDGMENTS

This material is based upon work supported by the National Science Foundation under Grant No. 2203340. The authors acknowledge funding from the Department of Chemistry and Biochemistry at Kennesaw State University through departmental start-up funds. The College of Science and Mathematics also is acknowledged for funding through the Birla Carbon Scholars Program, a summer undergraduate research experience possible thanks to the generous donation from Birla Carbon. The authors also acknowledge funding from the Office of Undergraduate Research at Kennesaw State University for the Undergraduate Research and Creative Activities (URCA) funds. The authors would like to acknowledge Kennesaw State University Academic Affairs for support of the NMR facility, which made possible the research necessary for the completion of this project. The Reynolds Research Group at Georgia Tech is acknowledged for generous access to film processing and characterization facilities. Dr. Austin Jones is acknowledged for assistance with high-temperature GPC and solar cell measurements. Andrew Bates is acknowledged for assisting with AFM measurements.

CONFLICT OF INTEREST STATEMENT

The authors do not declare any financial interests.

ORCID

REFERENCES

- [1] L. Lu, T. Zheng, Q. Wu, A. M. Schneider, D. Zhao, L. Yu, *Chem. Rev.* **2015**, *115*, 12666.
- [2] A. Salehi, X. Fu, D. H. Shin, F. So, Adv. Funct. Mater. 2019, 29, 1808803.
- [3] X. Li, K. Perera, J. He, A. Gumyusenge, J. Mei, J. Mater. Chem. C 2019, 7, 12761.

- [4] C. Gu, A.-B. Jia, Y.-M. Zhang, S. X.-A. Zhang, Chem. Rev. 2022, 122, 14679.
- [5] T. P. Osedach, T. L. Andrew, V. Bulović, *Energy Environ. Sci.* 2013, 6, 711.
- [6] R. Po, G. Bianchi, C. Carbonera, A. Pellegrino, *Macromolecules* 2015, 48, 453.
- [7] J. J. Rech, J. Neu, Y. Qin, S. Samson, J. Shanahan, R. F. Josey, H. Ade, W. You, *ChemSusChem* 2021, 14, 3561.
- [8] M. Moser, A. Wadsworth, N. Gasparini, I. McCulloch, Adv. Energy Mater. 2021, 11, 2100056.
- [9] J. Fu, P. W. K. Fong, H. Liu, C.-S. Huang, X. Lu, S. Lu, M. Abdelsamie, T. Kodalle, C. M. Sutter-Fella, Y. Yang, G. Li, Nat. Commun. 2023, 14, 1760.
- [10] I. McCulloch, M. Chabinyc, C. Brabec, C. B. Nielsen, S. E. Watkins, *Nat. Mater.* 2023, 22, 1304.
- [11] C. J. Brabec, A. Distler, X. Du, H.-J. Egelhaaf, J. Hauch, T. Heumueller, N. Li, Adv. Energy Mater. 2020, 10, 2001864.
- [12] W. Yang, W. Wang, Y. Wang, R. Sun, J. Guo, H. Li, M. Shi, J. Guo, Y. Wu, T. Wang, G. Lu, C. J. Brabec, Y. Li, J. Min, *Joule* 2021, 5, 1209.
- [13] M. Rimmele, Z. Qiao, J. Panidi, F. Furlan, C. Lee, W. L. Tan, C. R. McNeill, Y. Kim, N. Gasparini, M. Heeney, *Mater. Horiz.* 2023, 10, 4202.
- [14] M. S. Vezie, S. Few, I. Meager, G. Pieridou, B. Dörling, R. S. Ashraf, A. R. Goñi, H. Bronstein, I. McCulloch, S. C. Hayes, M. Campoy-Quiles, J. Nelson, *Nat. Mater.* 2016, 15, 746.
- [15] E. Ravindran, N. Somanathan, J. Mater. Chem. C 2017, 5, 4763.
- [16] B. Xu, I. Pelse, S. Agarkar, S. Ito, J. Zhang, X. Yi, Y. Chujo, S. Marder, F. So, J. R. Reynolds, ACS Appl. Mater. Interfaces 2018, 10, 44583.
- [17] I. Pelse, J. L. Hernandez, S. Engmann, A. A. Herzing, L. J. Richter, J. R. Reynolds, ACS Appl. Mater. Interfaces 2020, 12, 27416.
- [18] F. Zhao, J. Zhou, D. He, C. Wang, Y. Lin, J. Mater. Chem. C 2021, 9, 15395.
- [19] J.-R. Pouliot, F. Grenier, J. T. Blaskovits, S. Beaupré, M. Leclerc, Chem. Rev. 2016, 116, 14225.
- [20] R. M. Pankow, B. C. Thompson, Polymer 2020, 207, 122874.
- [21] J. T. Blaskovits, M. Leclerc, Macromol. Rapid Commun. 2019, 40, 1800512.
- [22] L. Ye, B. C. Thompson, J. Polym. Sci. 2022, 60, 393.
- [23] L.-J. Yang, N. Chen, X.-M. Huang, Y. Wu, H. Liu, P. Liu, L. Hu, Z.-F. Li, S.-Y. Liu, ACS Appl. Polym. Mater. 2023, 5, 7340.
- [24] M. Krzeszewski, B. Thorsted, J. Brewer, D. T. Gryko, J. Org. Chem. 2014, 79, 3119.
- [25] M. Krzeszewski, D. Gryko, D. T. Gryko, Acc. Chem. Res. 2017, 50, 2334.
- [26] B. Sadowski, K. Hassanein, B. Ventura, D. T. Gryko, Org. Lett. 2018, 20, 3183.
- [27] S. Hatanaka, T. Ono, Y. Yano, D. T. Gryko, Y. Hisaeda, Chem-PhotoChem 2020, 4, 138.
- [28] Y. Qin, C. Schnedermann, M. Tasior, D. T. Gryko, D. G. Nocera, J. Phys. Chem. Lett. 2020, 11, 4866.
- [29] M. Tasior, G. Clermont, M. Blanchard-Desce, D. Jacquemin, D. T. Gryko, Chem. Eur. J. 2019, 25, 598.
- [30] R. Orłowski, M. Banasiewicz, G. Clermont, F. Castet, R. Nazir, M. Blanchard-Desce, D. T. Gryko, *Phys. Chem. Chem. Phys.* 2015, 17, 23724.

- [31] A. Janiga, D. Bednarska, B. Thorsted, J. Brewer, D. T. Gryko, Org. Biomol. Chem. 2014, 12, 2874.
- [32] M. Krzeszewski, T. Kodama, E. M. Espinoza, V. I. Vullev, T. Kubo, D. T. Gryko, *Chem. Eur. J.* 2016, 22, 16478.
- [33] R. K. Canjeevaram Balasubramanyam, R. Kumar, S. J. Ippolito, S. K. Bhargava, S. R. Periasamy, R. Narayan, P. Basak, J. Phys. Chem. C 2016, 120, 11313.
- [34] R. Domínguez, N. F. Montcada, P. De La Cruz, E. Palomares, F. Langa, ChemPlusChem 2017, 82, 1096.
- [35] J. Wang, Z. Chai, S. Liu, M. Fang, K. Chang, M. Han, L. Hong, H. Han, Q. Li, Z. Li, *Chem. Eur. J.* 2018, 24, 18032.
- [36] Y. Zhou, M. Zhang, J. Ye, H. Liu, K. Wang, Y. Yuan, Y.-Q. Du, C. Zhang, C.-J. Zheng, X.-H. Zhang, Org. Electron. 2019, 65, 110.
- [37] K.-J. J. Bell, A. M. Kisiel, E. Smith, A. L. Tomlinson, G. S. Collier, Chem. Mater. 2022, 34, 8729.
- [38] K. A. Bartlett, A. Charland-Martin, J. Lawton, A. L. Tomlinson, G. S. Collier, *Macromol. Rapid Commun.* 2023, 45, 2300220.
- [39] M. Tasior, O. Vakuliuk, D. Koga, B. Koszarna, K. Górski, M. Grzybowski, Ł. Kielesiński, M. Krzeszewski, D. T. Gryko, J. Org. Chem. 2020, 85, 13529.
- [40] Q. Liu, S. E. Bottle, P. Sonar, Adv. Mater. 2020, 32, 1903882.
- [41] A. Pron, P. Berrouard, M. Leclerc, Macromol. Chem. Phys. 2013, 214, 7.
- [42] A. M. Hawks, D. Altman, R. Faddis, E. M. Wagner, K.-J. J. Bell, A. Charland-Martin, G. S. Collier, J. Phys. Chem. B 2023, 33, 7352.
- [43] C. M. R. Abreu, P. Maximiano, T. Guliashvili, J. Nicolas, A. C. Serra, J. F. J. Coelho, RSC Adv. 2016, 6, 7495.
- [44] R. M. Pankow, L. Ye, N. S. Gobalasingham, N. Salami, S. Samal, B. C. Thompson, *Polym. Chem.* 2018, 9, 3885.
- [45] R. M. W. Wolfe, J. R. Reynolds, Org. Lett. 2017, 19, 996.
- [46] J. Kuwabara, T. Yasuda, N. Takase, T. Kanbara, ACS Appl. Mater. Interfaces 2016, 8, 1752.
- [47] S.-Y. Jang, I.-B. Kim, Y. Kim, D.-H. Lim, H. Kang, M. Heeney, D.-Y. Kim, Macromol. Rapid Commun. 2022, 43, 2200405.
- [48] J. Kuwabara, K. Hiyaji, S. Guo, X. Jiang, T. Yasuda, T. Kanbara, *Polym. J.* 2023, 55, 395.
- [49] A. S. Dudnik, T. J. Aldrich, N. D. Eastham, R. P. H. Chang, A. Facchetti, T. J. Marks, J. Am. Chem. Soc. 2016, 138, 15699.
- [50] M. Wakioka, N. Torii, M. Saito, I. Osaka, F. Ozawa, ACS Appl. Polym. Mater. 2021, 3, 830.
- [51] J. Min, Z.-G. Zhang, S. Zhang, Y. Li, Chem. Mater. 2012, 24, 3247.
- [52] A. Efrem, K. Wang, T. Jia, M. Wang, J. Polym. Sci. Part A: Polym. Chem. 2017, 55, 1869.
- [53] K. Wang, H. Chen, X. Wei, H. Bohra, F. He, M. Wang, *Dyes Pigments* 2018, 158, 183.
- [54] H. Bohra, H. Chen, Y. Peng, A. Efrem, F. He, M. Wang, J. Polym. Sci. Part A: Polym. Chem. 2018, 56, 2554.
- [55] L. A. Estrada, J. J. Deininger, G. D. Kamenov, J. R. Reynolds, ACS Macro Lett. 2013, 2, 869.
- [56] C. Roux, M. Leclerc, Chem. Mater. 1994, 6, 620.
- [57] M. Leclerc, M. Fréchette, J.-Y. Bergeron, M. Ranger, I. Lévesque, K. Faïd, Macromol. Chem. Phys. 1996, 197, 2077.
- [58] I. Lévesque, M. Leclerc, Chem. Mater. 1996, 8, 2843.

- [59] Y. Liu, J. Zhao, Z. Li, C. Mu, W. Ma, H. Hu, K. Jiang, H. Lin, H. Ade, H. Yan, Nat. Commun. 2014, 5, 5293.
- [60] J. Wachsmuth, A. Distler, C. Liu, T. Heumüller, Y. Liu, C. M. Aitchison, A. Hauser, M. Rossier, A. Robitaille, M.-A. Llobel, P. O. Morin, A. Thepaut, C. Arrive, I. McCulloch, Y. Zhou, C. J. Brabec, H. J. Egelhaaf, Sol. RRL 2023, 7, 2300602.
- [61] J. Padilla, A. M. Österholm, A. L. Dyer, J. R. Reynolds, Sol. Energy Mater. Sol. Cells 2015, 140, 54.
- [62] Z. Qian, L. Galuska, W. W. McNutt, M. U. Ocheje, Y. He, Z. Cao, S. Zhang, J. Xu, K. Hong, R. B. Goodman, S. Rondeau-Gagné, J. Mei, X. Gu, J. Polym. Sci. B Polym. Phys. 2019, 57, 1635.
- [63] J. Heinze, B. A. Frontana-Uribe, S. Ludwigs, Chem. Rev. 2010, 110, 4724.
- [64] J. Bertrandie, J. Han, C. S. P. De Castro, E. Yengel, J. Gorenflot, T. Anthopoulos, F. Laquai, A. Sharma, D. Baran, Adv. Mater. 2022, 34, 2202575.
- [65] C. M. Amb, A. L. Dyer, J. R. Reynolds, Chem. Mater. 2011, 23, 397.
- [66] P. Cai, X. Xu, J. Sun, J. Chen, Y. Cao, RSC Adv. 2017, 7, 20440.
- [67] Z.-F. Yao, J.-Y. Wang, J. Pei, Prog. Polym. Sci. 2023, 136, 101626.
- [68] P. M. Beaujuge, S. V. Vasilyeva, S. Ellinger, T. D. McCarley, J. R. Reynolds, *Macromolecules* 2009, 42, 3694.
- [69] P. M. Beaujuge, C. M. Amb, J. R. Reynolds, Acc. Chem. Res. 2010, 43, 1396.
- [70] R. H. Bulloch, J. A. Kerszulis, A. L. Dyer, J. R. Reynolds, ACS Appl. Mater. Interfaces 2015, 7, 1406.
- [71] T. Chen, S. Li, Y. Li, Z. Chen, H. Wu, Y. Lin, Y. Gao, M. Wang, G. Ding, J. Min, Z. Ma, H. Zhu, L. Zuo, H. Chen, Adv. Mater. 2023, 35, 2300400.
- [72] T. A. Bull, L. S. C. Pingree, S. A. Jenekhe, D. S. Ginger, C. K. Luscombe, ACS Nano 2009, 3, 627.
- [73] X. Fan, J. Wang, H. Huang, H. Wang, ACS Photon. 2014, 1,
- [74] Z. D. Seibers, G. S. Collier, B. W. Hopkins, E. S. Boone, T. P. Le, E. D. Gomez, S. M. Kilbey, *Soft Matter* 2020, *16*, 9769.
- [75] C. Cabanetos, A. El Labban, J. A. Bartelt, J. D. Douglas, W. R. Mateker, J. M. J. Fréchet, M. D. McGehee, P. M. Beaujuge, J. Am. Chem. Soc. 2013, 135, 4656.

- [76] W. Li, K. H. Hendriks, A. Furlan, W. S. C. Roelofs, M. M. Wienk, R. A. J. Janssen, J. Am. Chem. Soc. 2013, 135, 18942.
- [77] M.-S. Su, C.-Y. Kuo, M.-C. Yuan, U. S. Jeng, C.-J. Su, K.-H. Wei, Adv. Mater. 2011, 23, 3315.
- [78] Z. Du, H. M. Luong, S. Sabury, P. Therdkatanyuphong, S. Chae, C. Welton, A. L. Jones, J. Zhang, Z. Peng, Z. Zhu, et al., Mater. Horiz. 2023, 10, 5564.
- [79] Y.-F. Ma, Y. Zhang, H.-L. Zhang, J. Mater. Chem. C 2022, 10, 2364.
- [80] R. Datt, Suman, A. Bagui, A. Siddiqui, R. Sharma, V. Gupta, S. Yoo, S. Kumar, S. P. Singh, Sci. Rep. 2019, 9, 8529.
- [81] F. Pierini, M. Lanzi, P. Nakielski, S. Pawłowska, O. Urbanek, K. Zembrzycki, T. A. Kowalewski, *Macromolecules* 2017, 50, 4972
- [82] J. Yuan, D. Liu, H. Zhao, B. Lin, X. Zhou, H. B. Naveed, C. Zhao, K. Zhou, Z. Tang, F. Chen, W. Ma, Adv. Energy Mater. 2021, 11, 2100098.
- [83] G. Zhang, J. Zhao, P. C. Y. Chow, K. Jiang, J. Zhang, Z. Zhu, J. Zhang, F. Huang, H. Yan, Chem. Rev. 2018, 118, 3447.
- [84] M. M. Mandoc, L. J. A. Koster, P. W. M. Blom, Appl. Phys. Lett. 2007, 90, 133504.
- [85] S. M. Hosseini, N. Tokmoldin, Y. W. Lee, Y. Zou, H. Y. Woo, D. Neher, S. Shoaee, Sol. RRL 2020, 4, 2000498.
- [86] R. Ma, M. Zeng, Y. Li, T. Liu, Z. Luo, Y. Xu, P. Li, N. Zheng, J. Li, Y. Li, R. Chen, J. Hou, F. Huang, H. Yan, Adv. Energy Mater. 2021, 11, 2100492.

SUPPORTING INFORMATION

Additional supporting information can be found online in the Supporting Information section at the end of this article.

How to cite this article: K.-J. J. Bell, S. Sabury, V. Phan, E. M. Wagner, A. M. Hawks, K. A. Bartlett, G. S. Collier, *J. Polym. Sci.* **2024**, 1. https://doi.org/10.1002/pol.20240093